Unexpected source of Fukushima derived radiocesium to the coastal ocean of Japan

Virginie Sanial[1], Ken O. Buesseler[2], Matthew A. Charette[3], Seiya Nagao[4]

1 Department of Marine Chemistry and Geochemistry, Woods Hole Oceanographic Institution, 266 Woods Hole Road, MS#25, Woods Hole, MA 02543, USA vsanial@whoi.edu

2 Department of Marine Chemistry and Geochemistry, Woods Hole Oceanographic Institution, 266 Woods Hole Road, MS#25, Woods Hole, MA 02543, USA kbuesseler@whoi.edu

3 Department of Marine Chemistry and Geochemistry, Woods Hole Oceanographic Institution, 266 Woods Hole Road, MS#25, Woods Hole, MA 02543, USA mcharette@whoi.edu

4 Low Level Radioactivity Laboratory, Institute of Nature and Environmental Technology, Kanazawa University, Japan seiya-nagao@se.kanazawa-u.ac.jp

Correspondence and requests for materials should be addressed to K.O.B. 266 Woods Hole Road MS#25 Department of Marine Chemistry and Geochemistry 508-289-2309 kbuesseler@whoi.edu.

Classification: Physical Sciences (Environmental Sciences)

Abstract

There are 440 operational nuclear reactors in the world, with approximately half situated along the coastline. This includes the Fukushima Dai-ichi Nuclear Power Plant (FDNPP), which experienced multiple reactor meltdowns in March 2011 followed by the release of radioactivity to the marine environment. While surface inputs to the ocean via atmospheric deposition and rivers are usually well monitored after a nuclear accident, no study has focused on subterranean pathways. During our study period, we found the highest cesium-137 (^{137}Cs) levels (up to 23,000 Bq m^{-3}) outside of the FDNPP site not in the ocean, rivers or potable groundwater, but in groundwater beneath sand beaches over tens of kilometers away from the FDNPP. Here, we present evidence of a previously unknown, ongoing source of Fukushima-derived ^{137}Cs to the coastal ocean. We postulate that these beach sands were contaminated in 2011 through wave and tide driven exchange and sorption of highly radioactive Cs from seawater. Subsequent desorption of ^{137}Cs and fluid exchange from the beach sands was quantified using naturally occurring radium isotopes. This estimated ocean ^{137}Cs source (0.6 TBq y^{-1}) is of similar magnitude as the ongoing releases of ^{137}Cs from the FDNPP site for 2013-2016, as well as the input of Fukushima-derived dissolved ^{137}Cs via rivers. Though this ongoing source is not at present a public health issue for Japan, the release of Cs of this type and scale needs to be considered in NPP monitoring and scenarios involving future accidents.

Keywords: Fukushima Dai-ichi Nuclear Power Plant accident, Cesium, Submarine Groundwater Discharge

Significance Statement

Five years after the Fukushima Dai-ichi Nuclear Power Plant accident, the highest radiocesium (^{137}Cs) activities outside of the power plant site were observed in brackish groundwater underneath sand beaches. We hypothesize that the radiocesium was deposited on sand mineral surfaces in the days and weeks after the accident through wave and tide driven exchange of seawater through the beach face. As seawater radiocesium concentrations decreased, this radiocesium reentered the ocean via submarine groundwater discharge, at a rate on par with direct discharge from the power plant and river runoff. This new unanticipated pathway for the storage and release of radionuclides to ocean should be taken into account in the management of coastal areas where nuclear power plants are situated.

\body On March 11th, 2011, a 9.0 magnitude Earthquake triggered a 15-m tsunami that inundated the FDNPP causing power loss, explosions, and reactor meltdowns, releasing a significant quantity of radionuclides into the atmosphere (1–3). More than 80% of the atmospheric fallout occurred over the ocean, with the highest deposition in the nearshore marine environment (4). In addition, direct liquid discharge of contaminated cooling water flowed into the ocean, making the FDNPP disaster the largest accidental input of radionuclides to the ocean (5).

Cesium-137 is an abundant fission product of nuclear power generation and nuclear weapons testing, which when released to the environment persists for decades due to its long half-life (30.2 y). The largest releases of Fukushima-derived ^{137}Cs took place within the first month of the accident. The ongoing sources to the ocean that are known include rivers and groundwater flow beneath the FDNPP, but these are by comparison more than 1,000 times smaller than the 2011 releases, though they have persisted nearly six years after the accident (4). Submarine groundwater discharge has been recognized as an important pathway for the transport of materials from the land to the ocean (6), yet this process has not been evaluated as an ongoing source of radionuclides to the coastal environment outside of the vicinity of the FDNPP.

Here, we present the first ^{137}Cs activities measured in groundwater collected underneath beaches up to 100 km away from the FDNPP (Fig. 1a). Eight beaches were visited between 2013 and 2015, with a more intensive sampling survey conducted in 2016 at Yotsukura beach, 35 km south of the FDNPP. Additional fresh groundwater and river samples were collected in the vicinity of the sandy beaches.

Results and Discussion

Dissolved (<0.45 μm) ^{137}Cs activities in beach groundwater spanned three orders of magnitude, with a maximum value of 23,000 ± 460 Bq m^{-3} (Fig. 1b; Table S1). For perspective, three of the Yotsukura beach groundwater samples were higher than the Japanese drinking water limit of 10,000 Bq m^{-3}, though no one is either exposed to, or drinks these waters, thus public health is not of primary concern here. Beach groundwater ^{137}Cs activities were generally higher than in

nearby seawater, rivers, natural spring, and groundwater wells used for irrigation. The ^{137}Cs activity in seawater rapidly decreased after the accident (7), and for the period of our study, the median seawater ^{137}Cs activity within 100 km of the coastline (excluding the FDNPP harbor) was 14 Bq m^{-3} (Fig. S1). In freshwater, dissolved ^{137}Cs activities ranged from below detection to 5.8 ± 0.2 Bq m^{-3} (Table S1). Thus, the ^{137}Cs activities in beach groundwater cannot be explained by conservative mixing between any known fresh water and seawater sources (8). It must therefore be sourced from ^{137}Cs-enriched beach sands.

Four sand cores were collected on Yotsukura Beach (Table S2). In sand located between the beach surface and 40 cm, the ^{137}Cs activity was relatively constant at 17 ± 4 Bq kg^{-1}. Below 40 cm, the ^{137}Cs activity increased with depth, reaching maximum values of 700 ± 60 Bq kg^{-1} (Fig. S2). The ^{137}Cs inventory in the longest core was 4.8 ± 0.6 × 10^5 Bq m^{-2}, and is a minimum estimate since we did not reach the bottom of the high activity layer. This is one order of magnitude higher than the largest recorded marine sediment inventory (0.73 ± 0.02 × 10^5 Bq m^{-2}; offshore of the FDNPP (9)), within a factor of four of terrestrial soil cores (20 × 10^5 Bq m^{-2}) from the restricted access area, and in excess of soils in the Yotsukura region (10^5 Bq m^{-2}) (10). Further, the deep enrichment of ^{137}Cs is inconsistent with a Fukushima atmospheric fallout source as ^{137}Cs would have likely been trapped in the upper layers of the sand horizon as demonstrated in land soils (10).

Consequently, we need to consider an alternative source to explain the high ^{137}Cs activities deeper in both beach sand and groundwater. In the days-weeks following the reactor meltdowns, dissolved ^{137}Cs activities reached > 60 × 10^6 Bq m^{-3} in the ocean offshore of the FDNPP (5). Numerical modeling demonstrated that a net southward flowing coastal current transported this highly radioactive seawater along the shoreline (11). We hypothesize that seawater intrusion, driven in part by waves and tides (12–15), led to the storage of ^{137}Cs by adsorption onto beach sands. In the years since the accident, falling ocean ^{137}Cs activities and similar groundwater-surface water exchange processes would have led to the reverse reaction (desorption) and the elevated beach groundwater ^{137}Cs activities observed today (Fig. 2). The ^{137}Cs enriched groundwater is then available to be released to the ocean via submarine groundwater discharge

(16, 17). The increasing ^{137}Cs activities in the surf zone with the falling tide (Fig. S3) is one line of evidence that the groundwater ^{137}Cs is discharged to the sea with tidal pumping.

To test this hypothesis, ^{137}Cs adsorption and desorption experiments were conducted on Japanese beach sand samples (Table S3; Fig. S4) with seawater solutions of varying salinities to reproduce the salinity gradient observed in beach groundwater. Seawater solutions were spiked with ^{137}Cs standard to reproduce the concentration of 1×10^6 Bq m^{-3} observed in April 2011 in the ocean off Iwasawa Beach, 16 km south of the FDNPP (5). The experiments showed that beach sands have an adequate ion exchange capacity for this level of ^{137}Cs, with an average adsorption fraction of 99% regardless of the salinity, sediment grain size, or mineralogy (Table S3). Desorption experiments involved recirculating ^{137}Cs free seawater through the beach sand. The desorption fraction ranged from 1.4% to 11.4%, with the highest values found at intermediate salinities except for one low salinity treatment with 22% desorbed ^{137}Cs (Fig. S4). These desorption rates were higher than those observed from riverine particles (18) or estuarine sediments (19), but consistent with a well-known property of Cs: decreasing solid-solution partitioning with increasing ionic strength (20). Therefore, beach sands appear to be capable of storing a large inventory of ^{137}Cs at depth that over time may be remobilized by seawater intrusion into beach aquifers and released to the coastal environment via groundwater-surface water exchange processes.

In beach settings, seawater intrusion generally follows two pathways: (i) an upper saline plume in the intertidal zone set up by waves and tides and (ii) a salt water wedge at depth, a function of the density difference between fresh groundwater and seawater (13, 15; Fig. 2). The sand cores and the groundwater samples were collected at depths less than 2 m, along the boundary of influence of a typical upper saline plume, which is characterized by dynamic mixing and exchange with seawater on time scales of days to weeks (13). The lower ^{137}Cs concentration in the shallow cores could thus be the result of more frequent flushing with seawater in comparison to the deeper sand layer, or less exposure to high ^{137}Cs activity seawater in 2011. The highly heterogeneous distribution of ^{137}Cs in beach groundwater is also supported by the complexity of upper saline plume dynamics (15) as well as variability in sand physical and biogeochemical properties as shown by the desorption experiments.

Regardless of the mechanisms controlling the concentration of ^{137}Cs in groundwater, beach aquifers in close proximity to FDNPP must be a source of ^{137}Cs to the ocean, which is supported by surf zone ^{137}Cs activities that were higher than offshore seawater during the study period (Fig. 1b). To quantify the magnitude of this ^{137}Cs source, we used parallel measurements of radium isotopes (^{223}Ra: 11.4 d, ^{224}Ra: 3.66 d), which are a well-established tool for providing regional scale estimates of submarine groundwater discharge (21, 22). Radium isotopes are continuously produced in aquifer sediments by the decay of insoluble thorium parent isotopes. Ra has a similar geochemical behavior to Cs and Ra activities were also significantly higher in brackish groundwater than fresh water or seawater (Fig. S5). Like ^{137}Cs, Ra activities in the surf zone were inversely correlated with tidal stage (Fig. S3). These characteristics are why Ra isotopes can be used as tracers of the ocean input of ^{137}Cs from beach groundwater.

A Ra isotope mass-balance model (21–24) for the surf zone was used to estimate the volume of ocean water that exchanges with the beach aquifer on a daily basis. In the model, we assume that submarine groundwater discharge is the only source of Ra to the surf zone, and that this source is balanced by Ra loss due to decay and mixing. The model was solved independently for the two Ra isotopes, which yielded a range of flux estimates between 0.07-0.51 $m^3\ m^{-2}\ d^{-1}$ for multiple beaches (Table S4).

To scale this estimate, we must make assumptions about the area over which the exchange of ^{137}Cs-rich beach groundwater is occurring. The highest FDNPP ^{137}Cs-contaminated marine sediments extend along 180 km of coastline (9). However, only ~45 % of the coastline is covered by sandy beaches (80 km). Assuming groundwater-surface water exchange occurs over a (shore perpendicular) intertidal zone width of 50 m (calculated from beach slope and tidal range), the exchange of water was estimated to be on the order of 3.0-20 $\times\ 10^5\ m^3\ d^{-1}$ (mean = $9.9 \times 10^5\ m^3\ d^{-1}$). Using the statistical mean of ^{137}Cs activity in beach groundwater 1520 ± 570 Bq m^{-3} (Fig. S6) and assuming a constant exchange of water over the period 2013-2016, we estimate that the amount of ^{137}Cs delivered by submarine groundwater discharge along the Japanese coastline is on the order of 0.2-1.1 TBq y^{-1}, with an average of 0.6 TBq y^{-1} ($T = 10^{12}$).

Terrestrial groundwater discharge to the ocean from the main island of Japan (Honshu) has been estimated at 44.5×10^3 m^3 d^{-1} km^{-1} (25), which is equivalent to 3.5×10^6 m^3 d^{-1} when scaled to our 80 km shoreline length. The ^{137}Cs activities were relatively low in terrestrial groundwater, 2.3 Bq m^{-3} on average in irrigation wells and in the natural spring, likely due to the strong affinity of Cs for clay particles in low ionic strength fluids, which limits its mobility in most inland freshwater aquifers (20). We estimate the amount of ^{137}Cs carried to the ocean by terrestrial groundwater to be on the order of 3×10^{-3} TBq y^{-1}, which is <1% of the flux of ^{137}Cs from brackish groundwater discharge. Thus, outside of the FDNPP site, the beach groundwater source dominates the flux of ^{137}Cs released to the coastal ocean via submarine groundwater discharge.

In comparison to other sources, the ongoing releases of ^{137}Cs at the FDNPP harbor were estimated to be 3 TBq y^{-1} for the summer 2012 (26). Harbor ^{137}Cs activities decreased by a factor of 5 between 2013 to 2016 (Fig. S1) (27). Therefore, assuming that the flushing rate of the harbor has remained constant, the present-day FDNPP harbor flux should be ~0.6 TBq y^{-1}. Another ongoing source of FDNPP derived ^{137}Cs is from rivers, with release estimates for total ^{137}Cs ranging from 2-12 TBq y^{-1} (28–31). Typhoons and heavy rain events have been shown to increase the river runoff flux; the ^{137}Cs input from this source is largely in the particulate phase (32), of which only a small amount is capable of entering the dissolved phase via desorption in the estuarine mixing zone (19). Thus, considering that ~90 % of the Cs is irreversibly bound to riverine suspended sediments (19), the riverine flux of dissolved ^{137}Cs is only ~0.2-1.2 TBq y^{-1}. Hence, the ocean input of ^{137}Cs from groundwater below the sandy beaches is similar in magnitude as the other two major sources, namely ongoing FDNPP and dissolved river sources. Similar to projected decreases in ^{137}Cs carried by run-off from land (30) and decreasing concentrations in the harbor at the FDNPP, the concentrations of ^{137}Cs in sand will likely diminish over time due to desorption, and thereby the beach source to the ocean is expected to become depleted.

This study demonstrates that, aside from the aquifer beneath the FDNPP, the highest recorded present day activities of ^{137}Cs in the aqueous environment in Japan are associated with brackish groundwater underneath beaches. This finding suggests that the beach sands served as a reservoir

for ^{137}Cs, which is subsequently released via submarine groundwater discharge to the ocean. Using Ra isotopes, we were able to make the first estimate of the magnitude of this flux, and found that it is similar to other ongoing sources, including export from the FDNPP harbor. This unexpected and ongoing ^{137}Cs source requires further investigation, in particular more systematic sampling in space and time given the variability in our groundwater and sand ^{137}Cs observations. The implications of our study extend well beyond the FDNPP event to siting of all coastal NPPs, and this source will need to be considered when evaluating the fate of radionuclides in the ocean from both intentional (e.g. Sellafield) and unanticipated releases.

Methods

Sampling

Field trips for groundwater sampling were conducted in May 2013, Sept 2013, Oct 2014, Oct 2015, and Nov 2016. The river samples came from the Natsui, Iwasawa, Kido, Niido, Mano, and the Same Rivers. Brackish groundwater samples were collected at Nobiru, Nagahama, Funatsuke, Kawahata, Yotsukura, Karasuzaki, Iwasawa, and Nakaso beaches using peristaltic pumps and 1-2 m-long push point piezometers (M.H.E. Products, Inc.). All water samples, including those from beaches, wells, rivers, and surf zones were filtered through a 0.45 μm pore sized filter. The water was then passed through a fiber impregnated with MnO_2 ("Mn-fiber") to pre-concentrate radium (33) directly in the field. The water samples were then stored on 20-L cubitainers to determine the Cs activities. Sediment profiles were obtained by digging pits on the beach and sampling the pit walls at 5 cm intervals.

Analysis

The beach sand samples were homogenized, dried, and counted on a gamma detector at the Low Level Radioactivity Laboratory in Kanazawa University (Table S2). The water samples were spiked with stable Cs and passed through columns filled with 5 mL of KNiFC－PAN ion-exchange resin (Czech Technical University, Prague) for the extraction of radiocesium (34). Column Cs efficiency was determined by measuring the stable Cs in the filtrate via ICP-MS. Yields were on average 98.8 ± 1.4% (STD). The yields are not determined yet for the samples collected in 2016, thus the average recovery was a considered. The resins were then dried, transferred into vials, and counted on a well-type small anode germanium (SAGe) gamma

246 detector from Canberra Industries with a cosmic veto suppression system to quantify the ^{137}Cs
247 activities using the gamma peaks at 661 keV and ^{134}Cs using gamma peaks at 605 and 795 keV
248 (35). All the Cs activities were decay corrected to the sampling date. Gamma detectors were
249 calibrated against internal standards and an International Atomic Energy Agency Irish Sea water
250 reference standard (IAEA-443; (36)).Though not discussed herein, ^{134}Cs was detected in all
251 samples (Table S1), indicative of a FDNPP source with a 1:1 release ratio due to the
252 characteristics of the power plant such as reactor design, fuel cycle, or age (5). Therefore, once
253 decay corrected to the accident date, the ^{134}Cs activities are similar to the ^{137}Cs activities, which
254 is the reason that they are not discussed at length herein.
255
256 The Mn-fibers were rinsed with MQ water, partially dried, and counted on a RaDeCC system
257 (37) as soon as possible after collection to determine the short-lived radium isotopes (^{223}Ra,
258 ^{224}Ra). Two additional counting sessions were conducted after 3 weeks to determine the ^{224}Ra
259 supported by ^{228}Th, and again after 3 months to determine the ^{223}Ra supported by ^{227}Ac. The
260 RaDeCC system was calibrated with standards prepared in the same geometry as the Mn-fiber
261 samples (37, 38).
262
263 **Adsorption-Desorption experiments conducted in beach sand samples**
264 Filtered seawater (1 μm pore size) from Cape Cod Bay (MA, USA) was used during the ^{137}Cs
265 adsorption and desorption experiments. The seawater was also processed through a KNiFC−PAN
266 ion-exchange resin in order to remove the background ^{137}Cs. The filtered seawater was diluted
267 with Milli-Q water to produce four solutions of salinity 4, 10, 20, and 30. Sand samples were
268 collected on two different beaches near the FDNPP (Table S1). The ^{137}Cs activities in the sand
269 were determined by gamma spectrometry.
270
271 The adsorption experiments were conducted on three sand samples (Table S3). Our experiment
272 was designed to reproduce the infiltration of groundwater through the beach sand. Briefly,
273 approximately 14 g of dry sand was placed into a column. Two 25 mL solutions, salinity 4 and
274 30, each with ^{137}Cs activities of 1,000,000 Bq m^{-3} were gravity filtered through the sand columns
275 two times with a filtration time of 15 min per sample. The filtrate was counted directly on a well-
276 type Germanium gamma detector to determine the fraction of ^{137}Cs adsorbed by the sand,

277 corrected for the amount of water retained by the sand (~5 mL). The ^{137}Cs adsorption fraction
278 ranged from 97.9-100 % with no correlation with salinity.
279
280 The desorption experiments were conducted on three sand samples (Table S3; Fig. S4).
281 Approximately 14 g of dry sand was placed into a column. Four 1 L solutions of salinity 4, 10,
282 20, and 30 were recirculated for 4 hours through the columns filled with sand using a peristaltic
283 pump at <10 ml min^{-1} in order to reproduce groundwater infiltration. The desorption experiments
284 were conducted in series on each sand starting with the low salinity solutions. The recovered
285 solutions containing the Cs desorbed from the sand were filtered (0.45 μm) and the ^{137}Cs
286 preconcentrated onto KNiFC−PAN. The resins were then dried, transferred into vials, and
287 counted on the gamma detector.
288
289 **Beach sand properties**
290 Grain size fractions and X-Ray diffraction analysis were conducted on the sand samples used in
291 the desorption experiments. The grain size fraction was relatively homogeneous throughout the
292 deepest sand core (105 cm) with a d50 average of 227 ± 14 μm (STD), which is classified as fine
293 sand. Clay (< 2 μm) and silt (< 60 μm) size fractions in the beach sand were negligible, though
294 X-ray diffraction analysis (Table S3; Fig. S4) indicated that the largest Cs desorption was
295 observed for the sand sample that had the greatest clay mineral content.
296
297 The distribution coefficient (K_d) for ^{137}Cs in beach sand can be estimated from the desorption
298 experiments using:
299 $$K_d = V_w\ (1-\alpha)/(M_s\ \alpha) \quad (1)$$
300 where, V_w is the volume of water used in the desorption experiment (1 L), M_s is the solid mass of
301 sand (14 g), and α is the desorption fraction. Considering a desorption fraction of 1.8% to 22%
302 (Fig. S4), the K_d values of the beach sand are between 250 L kg^{-1} and 3400 L kg^{-1}, which agree
303 with values previously observed for sediment-seawater interactions in Japanese coastal areas
304 before the FDNPP accident (39). Applying these K_d values to the ^{137}Cs concentrations measured
305 in the sand cores collected at Yotsukura permits a prediction of the concentrations in
306 groundwater from:

$^{137}Cs_{GW} = {}^{137}Cs_{sand} / K_d$ (2)

where $^{137}Cs_{GW}$ is the dissolved ^{137}Cs activity in groundwater and $^{137}Cs_{sand}$ is the ^{137}Cs activity in the sand. In the upper section, the mean $^{137}Cs_{sand}$ activity was 17 Bq kg^{-1}, which leads to a $^{137}Cs_{GW}$ of 4-70 Bq m^{-3}. In the deeper section, the mean $^{137}Cs_{sand}$ activity was 700 Bq kg^{-1}, which leads to a $^{137}Cs_{GW}$ of 180-2800 Bq m^{-3}. The majority of the ^{137}Cs activities measured in groundwater fall into the range of the $^{137}Cs_{GW}$ estimated from the K_d based on the desorption experiments (Fig. 1b), which supports our hypothesis that desorption from beach sand is the main mechanism releasing the ^{137}Cs in groundwater.

Cesium-137 flux from beach groundwater using a radium mass balance model

In order to estimate the flux of ^{137}Cs-enriched water to the ocean through submarine groundwater discharge, we constructed a radium isotope mass balance model. Submarine groundwater discharge was estimated for Iwasawa, Yotsukura, Karasuzaki, and Nakoso beaches, and was based on samples collected in 2015 and for Yotsukura beach in 2016 when both offshore and surf zone seawater Ra isotope data were available. The model assumes 1) that the system is at steady state, which is a fair assumption due to the fast production rate of short-lived radium isotopes (40), 2) that submarine groundwater discharge is the primary source of Ra to the surf zone (23, 24), in other words that diffusion from sediments is negligible, which we think is satisfied given the high-energy surf zone (41, 42), and 3) that this input is balanced by the loss of Ra due to decay and mixing (Eq. 3 and ref 22). For ^{224}Ra or ^{223}Ra, the model can be expressed as:

$F\text{-}Ra_{GW} = I\text{-}Ra_{SZ} (\lambda + 1/T)$ (3)

where, $F\text{-}Ra_{GW}$ is the groundwater flux of ^{224}Ra or ^{223}Ra, $I\text{-}Ra_{SZ}$ is the excess Ra inventory in the surf zone relative to the offshore water, λ is the decay constant of the Ra isotope considered, and T is the residence time of the water in the surf zone, which we assume to be equal to one tidal cycle (~0.5 d). The Ra_{SZ} were corrected for the average Ra activity in offshore water we measured from samples collected during two cruises conducted in 2015 (^{223}Ra: 7.1 dpm m^{-3} and ^{224}Ra: 80.5 dpm m^{-3}) and in 2016 (^{223}Ra: 2.9 dpm m^{-3} and ^{224}Ra: 48.1 dpm m^{-3}).

Based on equation 3, we calculated the area-normalized, volumetric flux of submarine groundwater discharge (V_{GW}) independently with the two Ra isotopes following:

$V_{GW} = (F\text{-}Ra_{GW} \times h)/Ra_{GW}$ (4)

where, Ra_{GW} is the mean radium activity in groundwater and h is the tidal amplitude. The tide amplitude varied between -1 cm to 179 cm during November 2016 at the Onahama tide gauge with an average of 90 ± 7 cm. We assumed that the tide amplitude, the residence time in the surf zone, as well as the Ra_{GW} are the same for the different beaches. Our groundwater samples were well distributed across the gradient of salinity, thus, the Ra activities in groundwater are representative of fluids comprising submarine groundwater discharge (Fig. S5). In such a case, the mean Ra activity in groundwater is equal to the statistical mean (bootstrap method) used to determine the mean ^{137}Cs activity in groundwater. Thus, we used the mean $^{223}Ra_{GW}$ and $^{224}Ra_{GW}$ activities in groundwater for salinities between 5 and 30 (like for Cs) of 105 ± 16 dpm m^{-3} and 1,990 ± 220 dpm m^{-3}, respectively, to quantify V_{GW}. For the four beaches, the submarine groundwater discharge fell in the range of 0.07-0.51 $m^3\ m^{-2}\ d^{-1}$ (Table S4).

In order to scale these area-normalized V_{GW} estimates to the affected region, we must calculate the area over which submarine groundwater discharge to the surf zone is occurring. As noted in the main body of the paper, we considered a coastline length of 180 km for which 80 km is covered by sand (estimated via Google Earth). During our sampling on November 15th, 2016, the tide covered 90 m of the Yotsukura beach, which coincided with an extreme lunar tide of 150 cm predicted at Onahama station (Fig. S3). Based on this observation, we estimated the slope of the Yotsukura beach face at 0.96°. Assuming that the beach slope was constant over the coastline length, the width of the intertidal cell is thus ~50 m for an average tide amplitude of 90 cm, and consistent with modeling studies of submarine groundwater discharge from beaches (15, 43). Note that this estimate could be a minimum width for the recirculation cell because submarine groundwater discharge occurs in the subtidal zone as well (44). This results in fluxes on the order of $3.0 \times 10^5\ m^3\ d^{-1}$ (using the min V_{GW}) and $20 \times 10^5\ m^3\ d^{-1}$ (using the max V_{GW}) with a mean flow of $9.9 \times 10^5\ m^3\ d^{-1}$.

Considering that the groundwater velocity flow was constant over the study period (2013-2016), the flux of ^{137}Cs due to submarine groundwater discharge is determined as follows:

$$F\ ^{137}Cs_{\ GW} = V_{GW} \times\ ^{137}Cs_{\ GW} \quad (5)$$

where, $^{137}Cs_{\ GW}$ is the statistical mean of ^{137}Cs activities in groundwater (Fig. S6).

ACKNOWLEDGEMENTS The authors are grateful to Aquamarine Fukushima, especially Kosuke Yoshida and Seiichi Tomihara for use of laboratory space and assistance with field sampling. We thank Maxi Castrillejo, Nuria Casacuberta, Steve Pike, Jessica Drysdale, Paul Henderson, Crystal Breier, Makio Honda, Hiroaki Saito, and Souichiro Terasaki for their help with logistics, field sample collection, and laboratory analyses. The authors are grateful to Andy Solow for his advice on statistics, and to Keisuke Fukushi, Frieder Klein, and especially Gabriela Farfan, for the X-ray Diffraction analyses. We thank the two anonymous reviewers for their constructive comments. V. Sanial was supported by a Postdoctoral Scholarship from the Center for Marine and Environmental Radioactivity (CMER). Funding for this work was provided by the Gordon and Betty Moore Foundation, the Deerbrook Charitable Trust, as well as the EC 7th Framework project COMET-FRAME (COordination and iMplementation of a pan-Europe instrumenT for radioecology) and KAKENHI (24110008).

Authors Contributions M.A.C. and K.O.B. co-designed the study. V.S., M.A.C., K.O.B. and S.N. performed research. S.N. analyzed the cesium in the sand core. V.S. and M.A.C. analyzed the radium in the water samples. K.O.B. analyzed the cesium in the water samples. V.S. led the writing of the manuscript with the contribution of all the co-authors.

References

1. Chino M, et al. (2011) Preliminary Estimation of Release Amounts of ^{131}I and ^{137}Cs Accidentally Discharged from the Fukushima Daiichi Nuclear Power Plant into the Atmosphere. *Journal of Nulcear Science and Technology* 48(7):1129–1134.

2. Morino Y, Ohara T, Nishizawa M (2011) Atmospheric behavior, deposition, and budget of radioactive materials from the Fukushima Daiichi nuclear power plant in March 2011. *Geophysical Research Letters* 38(7). doi:10.1029/2011GL048689.

3. Steinhauser G (2014) Fukushima's Forgotten Radionuclides: A Review of the Understudied Radioactive Emissions. *Environ Sci Technol* 48(9):4649–4663.

4. Buesseler K, et al. (2016) Fukushima Daiichi–Derived Radionuclides in the Ocean: Transport, Fate, and Impacts. *Annu Rev Mar Sci* 9(1):173–203.

5. Buesseler K, Aoyama M, Fukasawa M (2011) Impacts of the Fukushima Nuclear Power Plants on Marine Radioactivity. *Environ Sci Technol* 45(23):9931–9935.

6. Moore WS (2010) The Effect of Submarine Groundwater Discharge on the Ocean. *Annu Rev Mar Sci* 2(1):59–88.

7. Aoyama M, et al. (2016) ^{134}Cs and ^{137}Cs in the North Pacific Ocean derived from the March 2011 TEPCO Fukushima Dai-ichi Nuclear Power Plant accident, Japan. Part one: surface pathway and vertical distributions. *J Oceanogr* 72(1):53–65.

8. Boyle E, et al. (1974) On the chemical mass-balance in estuaries. *Geochim Cosmochim Acta* 38(11):1719–1728.

9. Black EE, Buesseler KO (2014) Spatial variability and the fate of cesium in coastal sediments near Fukushima, Japan. doi:10.5194/bg-11-5123-2014.

10. Lepage H, et al. (2015) Depth distribution of cesium-137 in paddy fields across the Fukushima pollution plume in 2013. *J Environ Radioact* 147:157–164.

11. Estournel C, et al. (2012) Assessment of the amount of cesium-137 released into the Pacific Ocean after the Fukushima accident and analysis of its dispersion in Japanese coastal waters. *J Geophys Res Oceans* 117(C11):C11014.

12. Li H, Boufadel MC, Weaver JW (2008) Tide-induced seawater–groundwater circulation in shallow beach aquifers. *J Hydrol* 352(1–2):211–224.

13. Xin P, Robinson C, Li L, Barry DA, Bakhtyar R (2010) Effects of wave forcing on a subterranean estuary. *Water Resour Res* 46(12):W12505.

14. Li X, Hu BX, Burnett WC, Santos IR, Chanton JP (2009) Submarine Ground Water Discharge Driven by Tidal Pumping in a Heterogeneous Aquifer. *Ground Water* 47(4):558–568.

15. Robinson C, Li L, Prommer H (2007) Tide-induced recirculation across the aquifer-ocean interface. *Water Resour Res* 43(7):W07428.

16. Taniguchi M (2002) Tidal effects on submarine groundwater discharge into the ocean. *Geophys Res Lett* 29(12):2–1.

17. Burnett WC, et al. (2006) Quantifying submarine groundwater discharge in the coastal zone via multiple methods. *Sci Total Environ* 367(2–3):498–543.

18. Takata H, et al. (2015) Remobilization of radiocesium on riverine particles in seawater: The contribution of desorption to the export flux to the marine environment. *Mar Chem* 176:51–63.

19. Yamasaki S, et al. (2016) Radioactive Cs in the estuary sediments near Fukushima Daiichi Nuclear Power Plant. *Sci Total Environ* 551–552:155–162.

20. Evans DW, Alberts JJ, Clark RA (1983) Reversible ion-exchange fixation of cesium-137 leading to mobilization from reservoir sediments. *Geochimica et Cosmochimica Acta* 47(6):1041–1049.

21. Charette MA, Buesseler KO, Andrews JE (2001) Utility of radium isotopes for evaluating the input and transport of groundwater-derived nitrogen to a Cape Cod estuary. *Limnol Oceanogr* 46(2):465–470.

22. Moore WS, Blanton JO, Joye SB (2006) Estimates of flushing times, submarine groundwater discharge, and nutrient fluxes to Okatee Estuary, South Carolina. *J Geophys Res Oceans* 111(C9):C09006.

23. Beck AJ, Rapaglia JP, Cochran JK, Bokuniewicz HJ (2007) Radium mass-balance in Jamaica Bay, NY: Evidence for a substantial flux of submarine groundwater. *Mar Chem* 106(3–4):419–441.

24. Garcia-Solsona E, et al. (2010) An assessment of karstic submarine groundwater and associated nutrient discharge to a Mediterranean coastal area (Balearic Islands, Spain) using radium isotopes. *Biogeochemistry* 97(2–3):211–229.

25. Zektser IS, Everett LG, Dzhamalov RG (2006) *Submarine Groundwater* (CRC Press).

26. Kanda J (2013) Continuing ^{137}Cs release to the sea from the Fukushima Dai-ichi Nuclear Power Plant through 2012. *Biogeosciences* 10(9):6107–6113.

27. Japan Atomic Energy Agency Database for Radioactive Substance Monitoring Data. Available at: http://emdb.jaea.go.jp/emdb/en/ [Accessed January 30, 2017].

28. Evrard O, et al. (2015) Radiocesium transfer from hillslopes to the Pacific Ocean after the Fukushima Nuclear Power Plant accident: A review. *J Environ Radioact* 148:92–110.

29. Yamaguchi M, Kitamura A, Oda Y, Onishi Y (2014) Predicting the long-term ^{137}Cs distribution in Fukushima after the Fukushima Dai-ichi nuclear power plant accident: a parameter sensitivity analysis. *J Environ Radioact* 135:135–146.

30. Pratama MA, Yoneda M, Shimada Y, Matsui Y, Yamashiki Y (2015) Future projection of radiocesium flux to the ocean from the largest river impacted by Fukushima Daiichi Nuclear Power Plant. *Sci Rep* 5. doi:10.1038/srep08408.

31. Yamashiki Y, et al. (2014) Initial flux of sediment-associated radiocesium to the ocean from the largest river impacted by Fukushima Daiichi Nuclear Power Plant. *Sci Rep* 4:3714.

32. Nagao S, et al. (2013) Export of ^{134}Cs and ^{137}Cs in the Fukushima river systems at heavy rains by Typhoon Roke in September 2011. *Biogeosciences* 10(10):6215–6223.

33. Moore WS, Reid DF (1973) Extraction of radium from natural waters using manganese-impregnated acrylic fibers. *J Geophys Res* 78(36):8880–8886.

34. Breier CF, et al. (2016) New applications of KNiFC-PAN resin for broad scale monitoring of radiocesium following the Fukushima Dai-ichi nuclear disaster. *J Radioanal Nucl Chem* 307(3):2193–2200.

35. Pike SM, et al. (2016) Improved gamma-spectroscopy of marine samples via low background small anode germanium well detector with cosmic veto suppression. *J Radioanal Nucl Chem* 307(3):2359–2364.

36. Pham MK, et al. (2011) A certified reference material for radionuclides in the water sample from Irish Sea (IAEA-443). *J Radioanal Nucl Chem* 288(2):603–611.

37. Moore WS (2008) Fifteen years experience in measuring ^{224}Ra and ^{223}Ra by delayed-coincidence counting. *Mar Chem* 109(3–4):188–197.

38. Scholten JC, et al. (2010) Preparation of Mn-fiber standards for the efficiency calibration of the delayed coincidence counting system (RaDeCC). *Mar Chem* 121(1–4):206–214.

39 Uchida S, Tagami K Comparison of coastal area sediment-seawater distribution coefficients (K_d) of stable and radioactive Sr and Cs. *Appl Geochem*. doi:10.1016/j.apgeochem.2016.12.023.

40. Webster IT, Hancock GJ, Murray AS (1994) Use of radium isotopes to examine pore-water exchange in an estuary. *Limnol Oceanogr* 39(8):1917–1927.

41. Precht E, Huettel M (2003) Advective pore-water exchange driven by surface gravity waves and its ecological implications. *Limnol Oceanogr* 48(4):1674–1684.

42. Street JH, Knee KL, Grossman EE, Paytan A (2008) Submarine groundwater discharge and nutrient addition to the coastal zone and coral reefs of leeward Hawai'i. *Marine Chemistry* 109(3):355–376.

43. Evans TB, Wilson AM (2016) Groundwater transport and the freshwater–saltwater interface below sandy beaches. *J Hydrol* 538:563–573.

44. Garcia-Solsona E, et al. (2008) Estimating submarine groundwater discharge around Isola La Cura, northern Venice Lagoon (Italy), by using the radium quartet. *Marine Chemistry* 109(3):292–306.

Figure captions

Figure 1. **Sample locations and ^{137}Cs activities near the Fukushima Dai-ichi Nuclear Power Plant (FDNPP). a**, Sample locations in the vicinity of the FDNPP. The seawater data (open squares) are from the Japan Atomic Energy Agency online database. The beach groundwater (GW), surf zone, and freshwater samples were collected between 2013 and 2016. **b**, ^{137}Cs activities determined in brackish groundwater underneath beaches, freshwater (irrigation wells and rivers), and seawater from the beach surf zones plotted vs salinity. The error bars are smaller than the symbols. The lines denote the ^{137}Cs Japanese drinking water (DW) limit, the median ^{137}Cs activity in seawater after the FDNPP accident (excluding the FDNPP harbor), and the ^{137}Cs activity level in seawater before the FDNPP accident.

Figure 2: Sources of Fukushima derived radiocesium to the coastal ocean off Japan in 2013-2016. As detailed in the text, the two known ongoing sources of dissolved ^{137}Cs include the FDNPP via flushing of its harbor (0.6 TBq y^{-1}) and river run off (0.2-1.2 TBq y^{-1}). We report here a previously unknown source of dissolved ^{137}Cs to the ocean from submarine groundwater discharge (SGD) along the Japan coastline of between 0.2-1.1 TBq y^{-1} (average 0.6 TBq y^{-1}). The main driving forces of submarine groundwater from beaches are waves (W), hydraulic head (H), tidal pumping (T), and convection (C). The southward flowing coastal current, represented by the light blue arrow, would have carried extremely high ^{137}Cs, some fraction of which was sorbed onto beach sands and later released as indicated by this study.

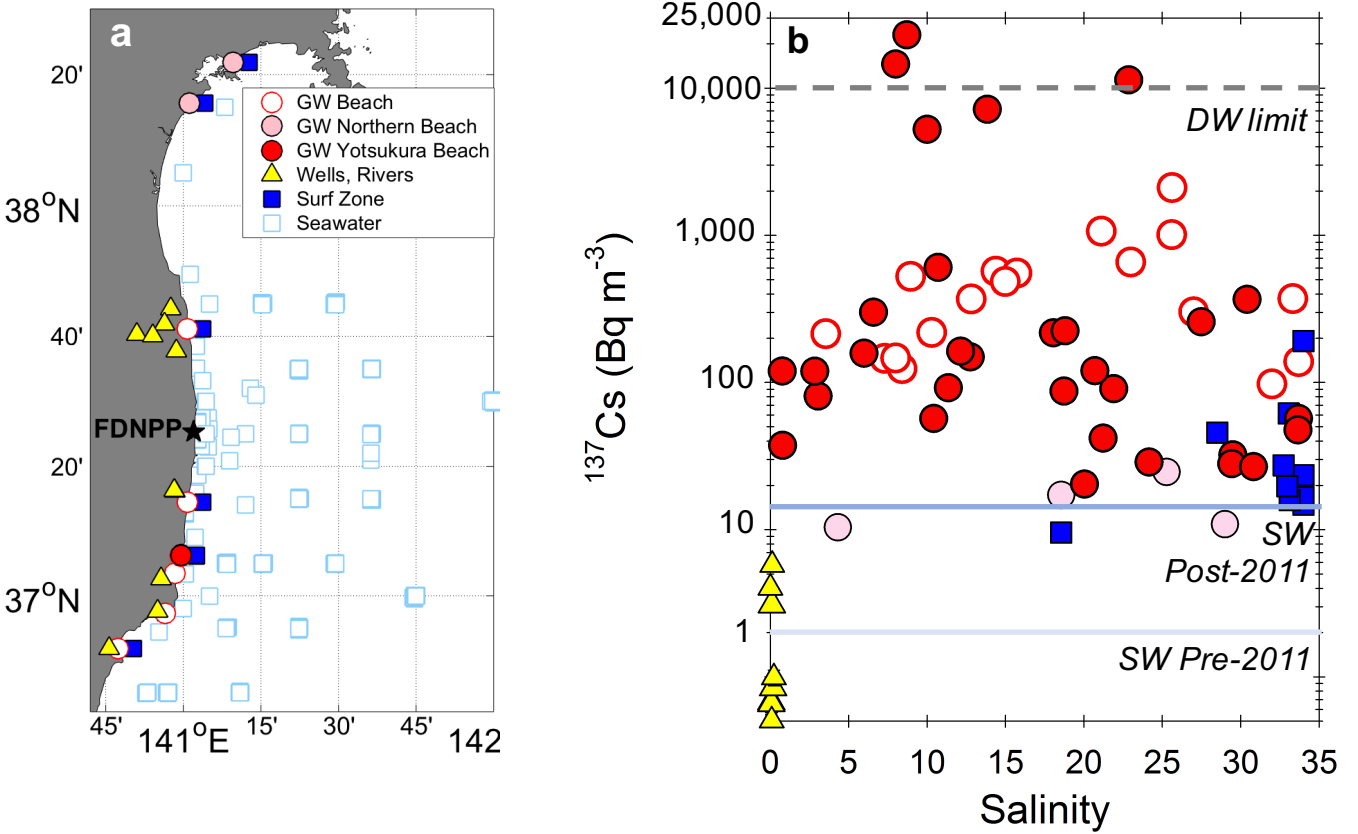
a
GW Beach
GW Northern Beach
GW Yotsukura Beach
Wells, Rivers
Surf Zone
Seawater
FDNPP
20'
38°N
40'
20'
37°N
45'
141°E
15'
30'
45'
142
b
25,000
10,000
1,000
100
10
1
DW limit
SW
Post-2011
SW Pre-2011
137Cs (Bq m-3)
0
5
10
15
20
25
30
35
Salinity

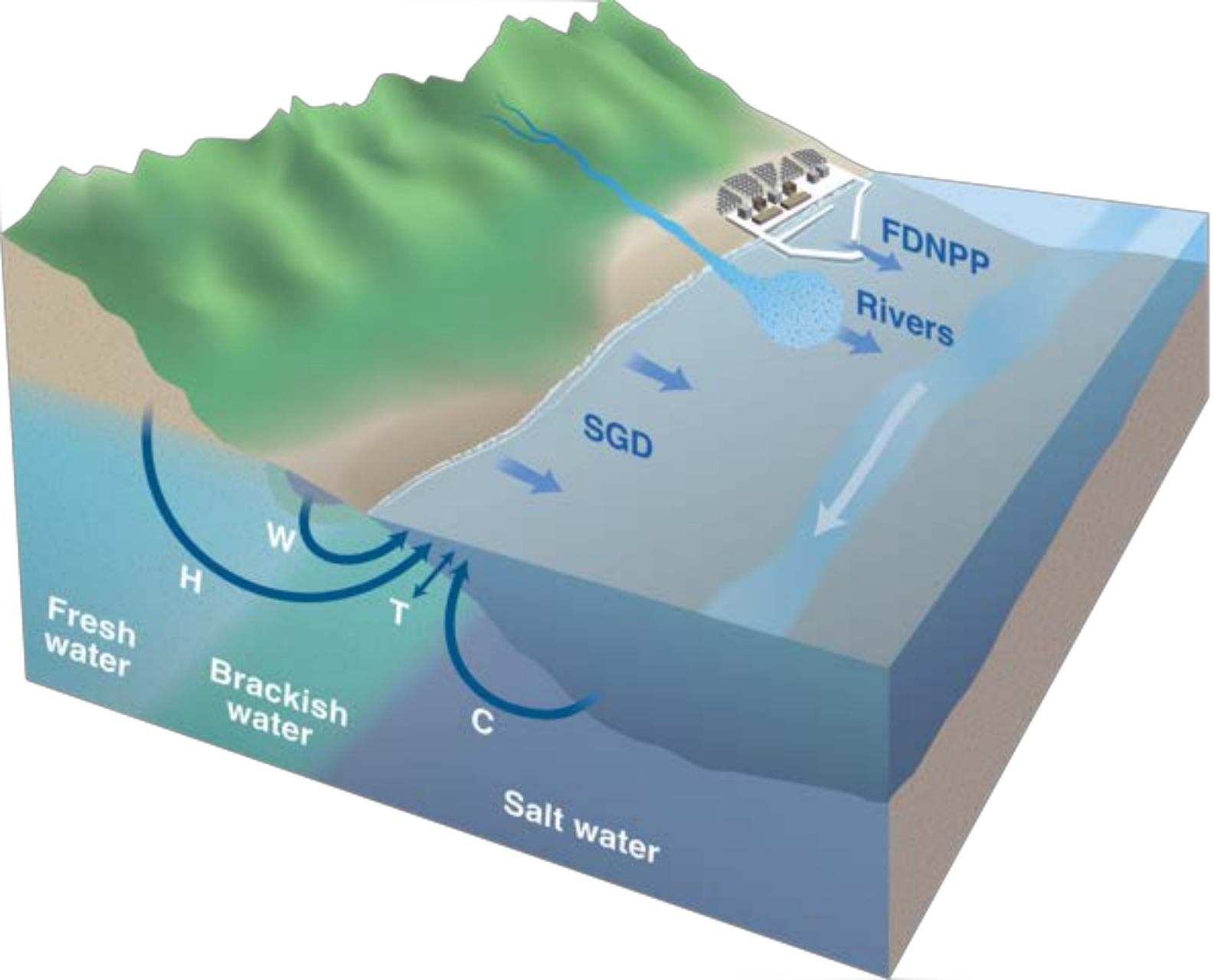
FDNPP
Rivers
SGD
W
H
T
C
Fresh water
Brackish water
Salt water

Table S1: Activities of dissolved ^{137}Cs and ^{134}Cs, and of ^{223}Ra and ^{224}Ra, in groundwater, river, irrigation well, natural spring, and surf zone samples collected between 2013 and 2016 in the vicinity of the Fukushima Dai-ichi Nuclear Power Plant (FDNPP). The Cs activities are decay corrected to the sampling date. ND (Not Determined). BDL (Below Detection Limit)

	Push point sampler length (m)	Distance from FDNPP (km)	Sampling Date	Lat (°N)	Lon (°E)	Salinity	^{137}Cs (Bq m^{-3})	^{134}Cs (Bq m^{-3})	^{223}Ra (dpm $100L^{-1}$)	^{224}Ra (dpm $100L^{-1}$)
Groundwater										
Funatsuke	2	50	5/17/13	36.955	140.944	33.7	138 ± 3	132 ± 3	11.5 ± 1.2	188.4 ± 4.2
	2		5/17/13	36.955	140.941	3.5	214 ± 4	203 ± 4	0.8 ± 0.1	19.6 ± 0.7
Kawahata	2	40	5/18/13	37.057	140.973	33.3	371 ± 7	351 ± 7	47.3 ± 4.4	877.5 ± 17.2
	2		5/18/13	37.057	140.973	8.4	124 ± 3	119 ± 3	6.0 ± 0.7	118.0 ± 2.5
Yotsukura	2	35	5/18/13	37.105	140.992	0.8	119 ± 2	114 ± 2	0.18 ± 0.1	7.0 ± 0.4
	2		10/15/14	37.104	140.992	8.0	14500 ± 300	5700 ± 100	2.7 ± 0.5	41.3 ± 1.1
	1		10/15/14	37.104	140.992	10.0	5200 ± 100	1690 ± 30	3.3 ± 0.3	123.0 ± 1.9
	1		10/18/15	37.104	140.992	10.7	600 ± 10	140 ± 3	5.5 ± 0.8	101.3 ± 2.8
	2		10/18/15	37.104	140.992	13.8	7200 ± 150	1660 ± 30	15.3 ± 1.6	236.0 ± 5.1
	1		10/18/15	37.104	140.992	22.9	11400 ± 200	2640 ± 50	20.1 ± 2.1	277.2 ± 6.2
	1		11/14/16	37.104	140.992	3.0	81 ± 2	13 ± 1	0.3 ± 0.1	16.6 ± 0.9
	1		11/14/16	37.104	140.992	18.1	217 ± 4	35 ± 1	5.6 ± 0.5	190.5 ± 2.4
	1		11/14/16	37.104	140.992	5.9	158 ± 3	25 ± 1	1.4 ± 0.2	50.1 ± 0.8
	2		11/14/16	37.103	140.992	30.4	366 ± 7	60 ± 1	13.7 ± 0.7	365.4 ± 3.3
	1		11/15/16	37.103	140.992	33.7	57 ± 1	9 ± 1	13.5 ± 0.9	403.9 ± 5.2
	1		11/15/16	37.103	140.992	33.7	48 ± 1	8 ± 1	16.6 ± 0.9	382.9 ± 4.0
	2		11/15/16	37.103	140.992	27.5	258 ± 5	41 ± 1	10.0 ± 0.7	286.1 ± 3.5
	2		11/15/16	37.104	140.992	18.8	224 ± 5	37 ± 1	5.3 ± 0.5	226.7 ± 3.3
	1		11/15/16	37.104	140.992	11.4	92 ± 2	15 ± 1	3.4 ± 0.4	89.3 ± 1.6
	1		11/15/16	37.104	140.992	6.6	299 ± 6	49 ± 1	1.2 ± 0.2	61.2 ± 1.4
	1		11/15/16	37.104	140.992	0.8	37 ± 1	6 ± 1	0.1 ± 0.1	2.5 ± 0.3
	2		11/16/16	37.103	140.991	21.9	91 ± 2	15 ± 1	7.2 ± 0.5	257.3 ± 2.1
	2		11/16/16	37.103	140.991	20.7	120 ± 2	20 ± 1	10.9 ± 0.6	281.6 ± 3.0

	2		11/16/16	37.103	140.991	21.2	42	±	1	6	±	1	4.6	±	0.5	186.6	±	3.0
	2		11/16/16	37.104	140.992	8.7	23000	±	460	3800	±	80	2.5	±	0.3	117.5	±	1.4
	1		12/1/16	37.103	140.992	20.0	20	±	1	3	±	1	11.2	±	1.2	163.7	±	4.6
	2		12/1/16	37.104	140.992	12.8	149	±	3	25	±	1	5.36	±	0.6	130.7	±	3.5
	1		12/1/16	37.104	140.992	2.8	119	±	2	19	±	1	0.5	±	0.2	24.5	±	2.0
	2		12/2/16	37.103	140.992	18.7	87	±	2	14	±	1	17.2	±	1.6	164.7	±	4.3
	1		12/2/16	37.103	140.992	29.5	32	±	1	5	±	1	17.7	±	1.4	295.8	±	3.8
	1		12/2/16	37.103	140.992	24.2	29	±	1	4	±	1	12.0	±	1.1	161.6	±	2.6
	1		12/2/16	37.103	140.992	29.4	28	±	1	4	±	1	10.8	±	2.0	219.6	±	8.9
	1		12/2/16	37.103	140.992	30.8	27	±	1	4	±	1	18.4	±	1.4	314.1	±	4.0
	1		12/2/16	37.104	140.992	10.4	57	±	1	9	±	1	5.3	±	0.7	72.3	±	2.5
	1		12/2/16	37.104	140.992	12.1	163	±	3	27	±	1	5.4	±	0.6	86.1	±	2.6
Nobiru	2	105	9/16/13	38.365	141.161	18.6	17	±	1	14	±	1	1.7	±	0.3	68.1	±	1.2
	2		9/16/13	38.365	141.161	4.3	10	±	1	11	±	1	0.4	±	0.1	4.3	±	0.3
Nagahama	2	90	9/16/13	38.261	141.020	25.3	25	±	1	23	±	1	4.8	±	0.9	104.0	±	2.3
	2		9/16/13	38.261	141.020	29.0	11	±	1	11	±	1	5.6	±	0.5	137.0	±	1.9
Iwasawa	1	20	10/19/15	37.241	141.013	0.9	45	±	1	10	±	1	0.8	±	0.1	10.7	±	0.3
	1		10/19/15	37.241	141.013	7.3	146	±	3	35	±	1	4.4	±	0.9	58.6	±	2.6
	1		10/19/15	37.241	141.013	12.8	368	±	8	85	±	1	8.3	±	1.3	106.1	±	3.7
	1		10/19/15	37.241	141.013	21.1	1060	±	20	250	±	5	48.4	±	2.8	560.0	±	7.8
	1		10/19/15	37.241	141.013	25.6	1000	±	20	240	±	5	28.3	±	2.3	399.0	±	6.5
Karasuzaki	2	30	10/20/15	37.686	141.013	10.3	218	±	4	52	±	1	2.4	±	0.4	71.8	±	1.4
	2		10/20/15	37.686	141.013	14.4	570	±	10	129	±	3	7.4	±	0.8	156.3	±	2.9
	2		10/20/15	37.686	141.013	15.7	550	±	10	126	±	3	10.4	±	1.1	149.8	±	3.1
	2		10/20/15	37.686	141.013	25.6	2100	±	40	489	±	11	9.7	±	1.1	207.3	±	3.8
Nakaso	1	65	10/22/15	36.864	140.790	8.9	530	±	10	126	±	3	11.7	±	1.3	251.9	±	5.0
	2		10/22/15	36.864	140.790	15.0	490	±	10	111	±	3	35.3	±	2.4	490.6	±	7.1
	2		10/22/15	36.864	140.790	23.0	660	±	10	147	±	4	50.3	±	3.1	574.1	±	8.1
	1		10/14/14	36.864	140.790	32.0	98	±	2	32	±	1	7.0	±	0.5	258.8	±	2.6
	2		10/15/14	36.864	140.790	8.0	150	±	3	57	±	1	7.8	±	0.6	177.2	±	2.0
	1		10/14/14	36.864	140.790	27.0	300	±	6	119	±	3	11.1	±	0.8	228.4	±	2.4

Table S1 Cont.

	Distance from FDNPP (km)	Sampling Date	Lat (°N)	Lon (°E)	Salinity	^{137}Cs (Bq m^{-3})	^{134}Cs (Bq m^{-3})	^{223}Ra (dpm 100L^{-1})	^{224}Ra (dpm 100L^{-1})
Rivers									
Natsui	31	10/18/15	37.671	140.881	0.1	0.67 ± 0.10	BDL -	BDL -	5.23 ± 0.34
Kido	17	10/19/15	37.272	141.000	0.0	0.49 ± 0.06	BDL -	0.09 ± 0.08	2.73 ± 0.22
Niido	31	10/20/15	37.698	140.969	0.1	0.66 ± 0.09	BDL -	BDL -	1.33 ± 0.14
Mano	29	10/20/15	37.668	140.932	0.1	3.08 ± 0.07	0.63 ± 0.08	0.13 ± 0.10	1.30 ± 0.26
Same	66	10/22/15	36.864	140.790	0.2	0.84 ± 0.08	BDL -	0.34 ± 0.19	3.23 ± 0.54
Irrigation wells									
Well 1	52	10/18/15	36.960	140.948	0.0	4.03 ± 0.12	0.90 ± 0.07	2.88 ± -	2.88 ± 0.22
Well 2	42	10/18/15	37.044	140.959	0.1	5.76 ± 0.22	1.14 ± 0.19	0.38 ± 0.09	4.87 ± 0.23
Well 3	17	10/19/15	37.270	141.004	0.1	0.51 ± 0.07	BDL -	1.25 ± 0.16	35.16 ± 0.64
Well 4	35	10/20/15	37.737	140.989	0.1	0.00 ± 0.00	BDL -	0.27 ± 0.14	0.22 ± 0.39
Natural spring	23	10/20/15	37.630	141.007	0.2	0.99 ± 0.12	BDL -	0.75 ± 0.13	18.46 ± 0.37
Surf zone									
Yotsukura	35	10/18/15	37.104	140.992	32.7	27.4 ± 0.58	5.9 ± 0.2	1.23 ± 0.1	28.90 ± 0.5
Yotsukura	35	11/15/16	37.103	140.992	33.2	23.4 ± 0.63	3.0 ± 0.2	2.21 ± 0.3	74.14 ± 1.1
Yotsukura	35	11/15/16	37.103	140.992	33.8	14.8 ± 0.38	1.9 ± 0.2	1.08 ± 0.2	43.75 ± 0.7
Yotsukura	35	11/15/16	37.103	140.992	33.8	16.6 ± 0.37	2.4 ± 0.1	1.82 ± 0.3	49.44 ± 1.2
Yotsukura	35	11/16/16	37.104	140.992	33.4	191.3 ± 3.94	32.0 ± 0.8	ND ± ND	ND ± ND
Nobiru	106	9/16/13	38.365	141.161	18.5	9.5 ± 0.22	8.1 ± 0.3	0.10 ± 0.1	15.90 ± 0.7
Nagahama	93	9/16/13	38.261	141.020	28.5	45.7 ± 1.24	38.4 ± 1.7	0.14 ± 0.1	1.53 ± 0.3
Iwasawa	20	10/19/15	37.241	141.013	33.1	61.6 ± 1.27	13.8 ± 0.3	3.20 ± 0.2	41.39 ± 0.7
Karasuzaki	29	10/20/15	37.686	141.013	33.1	15.9 ± 0.40	3.2 ± 0.2	1.13 ± 0.3	19.66 ± 0.9
Nakaso	66	10/22/15	36.864	140.790	33.0	19.7 ± 0.47	4.4 ± 0.2	1.90 ± 0.4	35.29 ± 1.4

Table S2: Activities of ^{137}Cs and ^{134}Cs in sand. The sand cores were collected at Yotsukura beach on November 2016. The activities are decay corrected to the sampling date and are expressed per kilogram of dry sand.

Core	Depth layer (cm)	^{137}Cs (Bq kg^{-1})	Err ^{137}Cs (Bq kg^{-1})	^{134}Cs (Bq kg^{-1})	Err ^{134}Cs (Bq kg^{-1})
1	0-5	17.3	0.4	2.8	0.2
	5-10	22.7	0.3	3.9	0.2
	10-15	23.2	0.3	3.7	0.1
	15-20	17.8	0.4	3.0	0.2
	20-25	22.5	0.2	4.0	0.1
	25-30	24.4	0.3	4.1	0.2
	30-35	24.3	0.9	4.7	0.5
	35-40	19.0	0.3	3.1	0.1
	40-45	16.8	0.3	2.7	0.2
	45-50	17.9	0.2	2.9	0.1
	50-55	19.8	0.4	3.0	0.2
	55-60	22.8	0.4	3.6	0.2
	60-65	29.4	0.3	4.9	0.1
	65-70	36.2	1.0	5.9	0.5
	70-75	47.7	1.4	7.8	0.6
	75-80	55.2	1.3	9.0	0.6
2	0-5	15.3	0.2	2.6	0.1
	5-10	16.9	0.4	2.7	0.2
	10-15	13.2	0.3	2.2	0.2
	15-20	12.4	0.5	2.0	0.2
	20-25	16.4	0.3	3.0	0.2
	25-30	18.8	0.6	3.0	0.3
3	0-5	13.6	0.3	2.3	0.1
	5-10	11.9	0.2	1.7	0.1
	10-15	11.4	0.3	2.1	0.1
	15-20	11.2	0.3	2.1	0.2
	20-25	11.8	0.3	2.0	0.1
	25-30	16.8	0.4	2.7	0.2
	30-35	24.8	0.4	3.9	0.2
	35-40	26.7	0.8	3.8	0.3
4	0-5	15.0	0.6	2.5	0.0
	5-10	15.3	0.3	2.6	0.0
	10-15	16.2	0.4	2.7	0.1
	15-20	16.5	0.3	2.8	0.1
	20-25	15.9	0.4	2.5	0.1
	25-30	14.4	0.6	2.6	0.1
	30-35	17.1	0.1	2.7	0.0
	35-40	19.9	0.0	3.3	0.3
	40-45	18.6	0.0	2.9	0.1
	45-50	24.0	0.5	4.2	0.1
	50-55	25.8	0.6	4.5	0.3
	55-60	37.1	1.7	6.2	0.3
	60-65	40.9	0.8	5.8	0.5
	65-70	28.6	0.3	4.6	0.6
	70-75	72.7	0.9	11.8	0.2
	75-80	580	2	98	1
	80-85	940	1	143	2
	85-90	960	20	160	5
	90-95	860	7	156	1
	95-100	600	10	105	1
	100-105	970	1	170	1

Table S3. Locations and ^{137}Cs (Bq kg^{-1}) activities of sand samples used in the adsorption desorption experiments.

Beach Name	Sand ID	^{137}Cs activity (Bq kg^{-1})	Err ^{137}Cs (Bq kg^{-1})	Mineral phase name content (%)							
				Quartz	Err	Clays	Err	Albite	Err	Aragonite	Err
Funatsuke	A	54	4	52	5	16	11	26	20	5	11
Yotsukura	B	94	7	42	6	27	6	21	3	10	3
Yotsukura	C	270	20	14	3	52	16	24	2	10	2

Clay minerals include Muscovite and Montmorillonite from the Mica and Smectite groups, respectively.

Table S4. Volumetric input of submarine groundwater discharge (V_{GW}) estimated using a ^{223}Ra and ^{244}Ra mass balance for the different beaches based on data collected in 2015 and 2016.

V_{GW} (m^3 m^{-2} d^{-1})	^{224}Ra	^{223}Ra
Iwasawa beach 2015	0.33	0.44
Yotsukura beach 2015	0.21	0.09
Karasuzaki beach 2015	0.12	0.07
Nakoso beach 2015	0.27	0.21
Yotsukura beach 2016	0.51	0.24